Characterization of Downflowing High Velocity Fluidized Beds

Chunshe Cao and Herbert Weinstein
Dept. of Chemical Engineering, The City College of New York, New York, NY 10031

A downer-riser circulating high velocity fluidization apparatus was developed to study the fundamentals of downflowing gas-solid particle mixtures. The acceleration and deceleration of solids due to the influences of the entrance and exit sections result in a relatively uniform axial solids distribution. Radial solid density profiles detected with an X-ray imaging system in the downer show the existence of a core-annulus flow with a dilute core surrounded by a denser wall region. Local solids flux profiles were obtained with an aspirating probe device and the solid velocity profile obtained from the two measured quantities. These confirm that the majority of solids segregates in a wall region that flows faster than the dilute core region. Thus, the shorter residence time in the high-speed downer wall region is coupled with faster reaction rates due to the accompanying high concentration of catalyst, while the dilute core has slower reaction rates with longer residence time due to the lower catalyst concentration and flow velocity. This results in much more uniform reaction extent over the cross-sectional area of the downer and, therefore, should improve the product selectivity.

Introduction

Reactor performance criteria such as yield and selectivity are typically adversely affected by backmixing in short contact time or residence time processes. These processes are typically catalytic or thermal cracking processes in which both the overcracking and the undercracking that result from backmixing provide very low value products. As unit residence times become shorter, the backmixing inherent in the conventional upflow riser system becomes more critical in limiting process yields and selectivity. The significant gas and solids backmixing is a result of the radially and axially nonuniform gas and solids flow. The core-annulus radial structure and the axially nonuniform density of the suspension in the upflow riser, which result in the backmixing and reduced contacting between the two phases, are due in part to the flow opposing the direction of the gravitational field.

It has been proposed that a reactor-reaction scheme utilizing a gas-solid mixture downflow concept would minimize backmixing and achieve a closer approach to the plug-flow condition in the reactor. When both the gas and solids flow directions are downwards, in the same direction as gravity, backmixing is expected to be essentially limited to the gas-solid mixing section at the upstream end and the gas-solid separation section at the downstream end. The proposed advantages of the downer reactor come from the fact that particles are cocurrently flowing downwards with the gas phase in the direction of the gravitational force, rather than against it, as in conventional riser reactors.

The application of gas-solid cocurrent downflowing high velocity fluidized beds would be particularly attractive in newly proposed industrial processes with very short residence times such as advanced catalytic cracking (Gartside, 1989; Murphy, 1992) if the backmixing is as limited as is anticipated. At present, only a limited number of studies have been reported on the fundamentals of downers. The research was pioneered by Shimizu et al. (1978) and followed by Aubert et al. (1994), Herbert et al. (1994), and Roques et al. (1994) in small diameter units. A series of hydrodynamic experiments were carried out by Jin's group (Wang et al., 1992; Cao et al., 1994; Wei et al., 1994) in a 14-cm modified riser-downer combination unit. Work on the formation of homogeneous downflow gas/solid suspensions at high velocities was reported more recently (Zenklusen et al., 1997). This literature,

Correspondence concerning this article should be addressed to H. Weinstein.
Current address of C. Cao: Exxon Mobil Research and Engineering Company, Clinton Township, Annandale, NJ 08801.

while significant, does not provide, however, a sufficient database for the properties of high velocity downflow of gas-solid powder mixtures upon which a process development can be based. Furthermore, evaluation methods for the backmixing level do not at present exist. In this investigation, an X-ray image visualization system and a local solids flux measurement device, as well as fast response pressure transducers, were used to provide flow quantities in a high velocity downer from which a partial assessment of downer suitability can be obtained.

Experimental Studies

This investigation was conducted in the City College downer-riser circulating fluidization unit, which includes two linked parallel tubes serving as downer and riser, a storage tank, a solid feed device, and a gas-solids separation system. The bed material used for the entire investigation was a Grace Davison fluid cracking catalyst, which has a particle density of 1,480 kg/m^3 and mean diameter of 82 μm. The system is shown in Figure 1. The downer consists of a Plexiglas tube with an inner diameter of 12.7 cm and a length of 4.6 m. A solid feeder wye which links the solids reservoir and a gas distributor with the downer tube configures the gas-solid entrance design. The vertical gas feed tube is also of 12.7-cm diameter and is coaxial with the downer. It contains flow straightening tubes. The solids fall from a fluidized bed through the other leg of the wye, which is at an angle of about 35° from the vertical. This is the simplest possible inlet design and is commercially feasible. The solids are carried down by the main air supply to a U-bend section, which connects the downer with the riser. The fluidizing medium is ambient air. Additional air which can be regulated separately over four independent air supply lines through five nozzles enters the system in the U-bend section. The additional air helps to blow the solids up through the riser to the reservoir above the solid feeder. The riser is also made of Plexiglas with a height of 8.85 m and the same diameter as that of the downer. The solid particles are carried up through the riser, which terminates in a flexible nylon tube feeding the primary cyclone. The primary cyclone is located in the top of the reservoir. The Plexiglas reservoir vessel (0.3048 m in ID; wall thickness 1.27 cm) is used as a storage bed for the solid. The solids separated in the primary cyclone fall down along the wall of the storage bed, which is kept at bubbling fluidization conditions. After passing through the secondary cyclone (Fisher-Klosterman Cyclone Collector), the air is exhausted through a bag filter which collects the fines. These fines are periodically returned to the reservoir. The separated solids from the secondary cyclone return to storage through a standpipe. A butterfly valve, which is located in the middle of the storage bed, is made out of a sintered plate. It is used to measure the solid flow rate when it is closed. It has negligible influence on the pressure balance of the circulating system. The change in differential pressure between tap 13 and 14 is recorded with the data acquisition system after closing the butterfly. When this valve is closed, the solids fluidize above the sintered plate and the bed below is carried away. The decay of the pressure drop due to the disappearing lower bed can be determined by applying linear regression to a 30 s record length of ΔP measurements taken at 100 Hz. The storage bed is kept in a steady fluidized condition during the measurement. The mass-flow rate of the fluidized solid between these two taps can be calculated with the rate of change of the pressure drop (Schnitzlein and Weinstein, 1988).

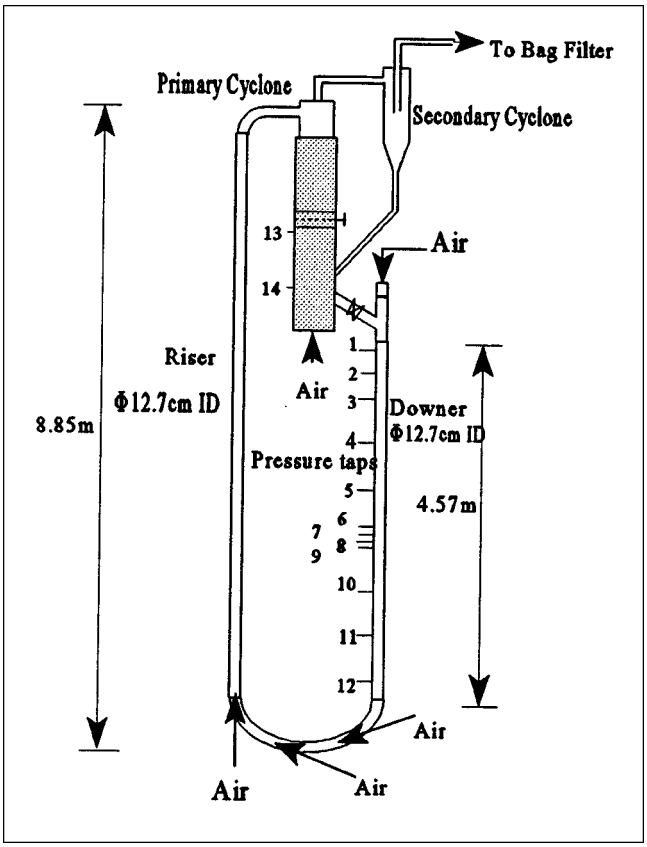

Figure 1. Downer-riser circulating fluidization unit.

Pairs of pressure taps installed at different heights were connected across pressure transducers and were hardwired to an A/D board mounted in the PC. In order to prevent blockages, purge air was passed continuously through the taps during fluidization.

An X-ray absorption system was used to give the solid fraction distribution. Continuous high intensity X-rays passed through the bed onto an image intensifier screen, which converted the X-rays into visible light. The light was focused on another screen equipped with a phototransistor array. The output electrical signals were sampled with the data acquisition system at the rate of 100 Hz. The X-ray absorption system gave a clear picture of the solids flow in the downer, and the radial solids fraction was obtained by image reconstruction along with a calibration. The details of the X-ray system and the calibration procedures are described in Feindt (1990).

A nonisokinetic sampling probe (Monceaux et al., 1985; Rhodes et al., 1988) was used to measure the local solid flux in the downer. The sampling device is shown in Figure 2. The sampling probe is 7.54 mm ID and 9.54 mm OD. The solids in the downer were aspirated with a vacuum through the sampling probe into a 1.22 m tall and 7.62 cm ID fluidized bed, which was maintained just above minimum fluidization. The top of the bed was a sintered plate to separate the solids and gas. Two pressure taps were installed along the bed to

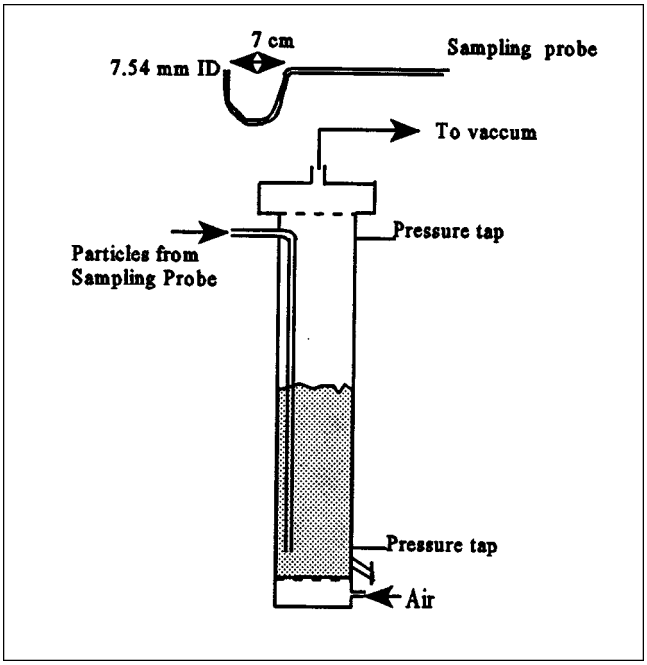

Figure 2. Local solid flux measurement device.

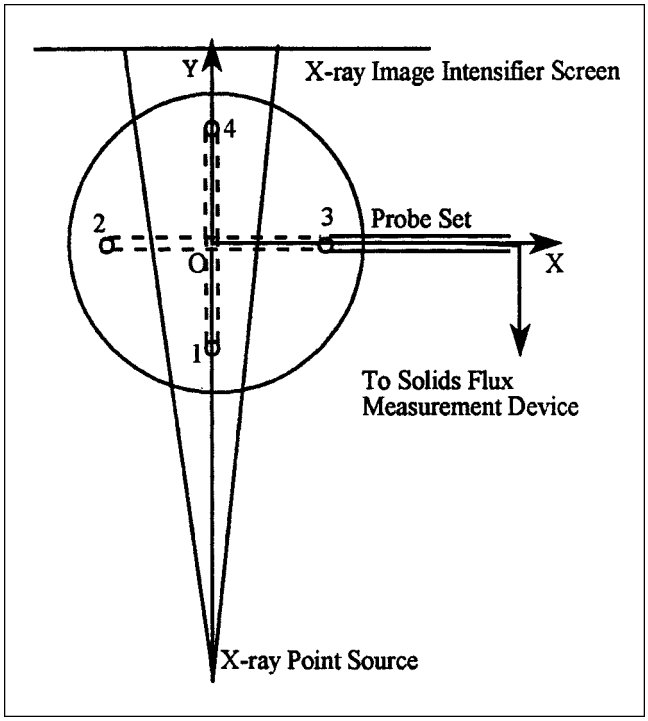

Figure 3. Cross-section of the downer with the solids downflow flux measurement probe set.

measure the increase of the pressure difference with time due to the addition of the solids from the aspirating probe. The increasing rate of the pressure difference gave the solid flux by

$$G_s(r/R) = \frac{A_{\text{samplingbed}}}{A_{\text{probe}}} \frac{1}{g} \frac{d(\Delta P)}{dt} \qquad (1)$$

where $G_s(r/R)$ is the local solid flux (kg/m^2·s), $A_{\text{samplingbed}}$ is the cross-sectional area of the sampling bed, and A_{probe} is the cross-sectional area of the sampling probe.

The probe was traversable along the radial direction of the bed. The aspirating velocity was kept as small as possible to ensure smooth suction flow from the downer. Rotating the probe 180 degrees to make the probe face downwards did not change the elevation of the probe location in the bed due to the configuration of the probe. It was necessary to measure the solids flow rate with the probe tip facing both upwards and downwards, and take the difference in order to eliminate the nonisokinetic sampling effect. A test to insure that the net rate of solids aspirated was independent of the aspirating velocity over the range employed was conducted (Kostazos, 1997). Furthermore, the integral of the measured flux over the cross-section was always compared to the independently measured circulation rate. Agreement was always within $\pm 11\%$.

Measurements of radial solid density with the X-ray imaging technique indicated that the solids distribution in the downer was asymmetric in the r-direction within the solids entrance region, and became symmetric about 1.2 m below the solids inlet (Cao, 1998). To verify the existence of axial symmetry below 1.2 m, a set of flux probes was designed to measure the solids downflow flux at four points in the cross-sectional area of the downer at 1.83 m, as shown in Figure 3.

These four measured points were located at the same elevation of the downer and at the same radial position. As shown in Figure 4, the solids downflow flux could be considered to be axially symmetric after the solids entrance region.

Results and Discussion

Pressure profile

The axial pressure profile is presented in Figure 5, in which L is the distance (m) from the solids entrance. The measurements indicate a ''bow'' shape distribution of the pressure in a gas-solids downflow fluidized bed. The results show the

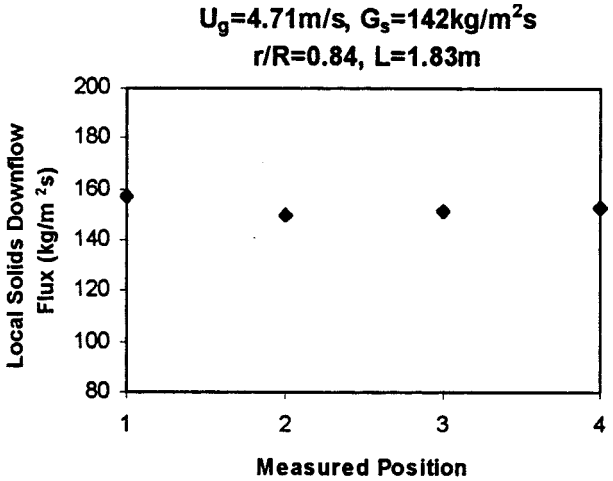

Figure 4. Demonstration of solids axial symmetry.

pressure first decreasing from the flow inlet downwards along the axial direction, then increasing gradually to the highest point at the bottom of the downer. The pressure gradient changes sign from negative to positive along the flow path. The location of the minimum pressure depends on the operating conditions.

The one-dimensional (1-D) momentum equation for the gas-solid flow in the downer can be expressed as

$$\frac{dP}{dx} = \rho_p g(1-\epsilon) - G_s \frac{dU_p}{dx} - \frac{dP_f}{dx} \qquad (2)$$

where x is the direction of the flow (the direction of gravity), and dP_f/dx is the frictional pressure drop. The terms of the righthand side of Eq. 2 represent the gravitational effects, the solid acceleration, and the frictional effects on the pressure gradient, respectively. The competition between these terms in the above expression can be seen in the experimental results. When particles enter the downer reactor, they accelerate to a high velocity driven by the gravity and gas drag forces. The second term $G_s(du_p)/(dx)$ is thus positive and large. The negative pressure gradients indicate the predominance of solid acceleration and friction over gravity head. In the process of acceleration, the slip velocity decreases rapidly, going through zero and eventually becoming negative, and the acceleration effects decline compared with those due to gravity. When $G_s(du_p)/(dx)$ decreases to the extent that the gravity becomes predominant, the pressure head begins to increase. Because of the restriction of the U-bend structure and the pressure balance requirement of the circulating system, the particle velocity will decrease before reaching the U-bend section. This deceleration of the particles results in a large increase of the pressure. In general, the minimum pressure point ($dp/dx = 0$) is typically located between 0.5 and 1.5 m from the entrance for this downer-riser loop configuration.

As shown in Figure 5a, in the higher solid flux case, the pressure at the bottom of the downer is relatively high due to the accumulation of particles just above the U-bend section. The absolute value of the pressure is higher for the higher solids flux cases since more dynamic power is needed to transport denser suspensions back up the riser. It also can be seen from Figure 5b that the absolute value of the pressure is higher at higher superficial gas velocity with the same solid circulation rate. The larger pressure head required to overcome the resistance of the entire flow system in the higher gas velocity operating case results in a higher-pressure value everywhere in the system than that in the lower gas-flow rate case.

Solid fraction profile

Figure 6 shows the radial solid density profiles at one elevation in the downer bed. They indicate a segregation of the two-phase flow as also occurs in a riser with a dilute core region surrounded by a dense annular wall region. The shape of the solid fraction profile is parabolic in the dense region and is flatter in the dilute region. Such a solid distribution is typical and independent of the operating conditions for the $L/D = 35$ downer used in this investigation. However, Figure 6 also shows that the larger the solid/gas ratio, the denser is the bed based on a cross-sectional area average.

The nonuniform radial solid distribution in downers was reported by other researchers using γ-ray absorptometry or fiber optic probes (Herbert et al., 1994; Zenklusen et al., 1997; Bai et al., 1991). Comparison of the results between this work and the others is shown in Figure 7. It can be observed that the solid fraction exhibits a larger value near the column wall than in the central region of the downers in all the reports. Note that the Zenklusen et al. (1997) experiment was carried out with a very dilute gas-solid suspension even if in a big column. He claimed that ''homogenous'' flow had been

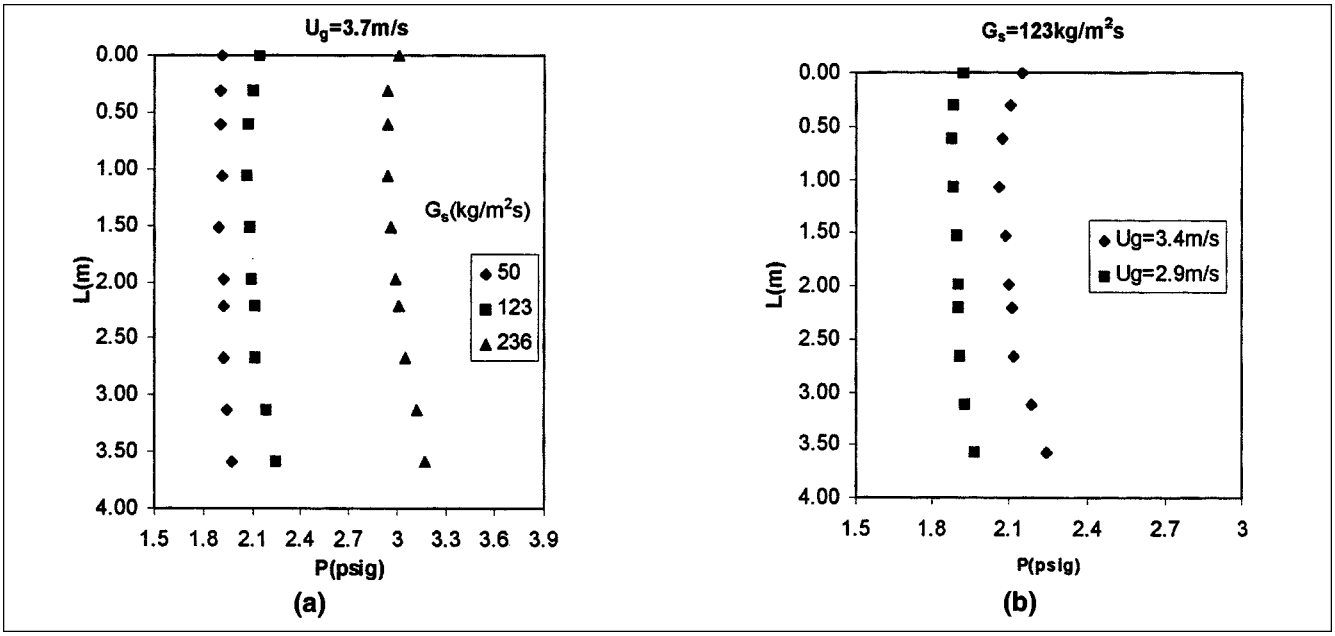

Figure 5. Pressure profiles.

(a) Constant gas velocity; (b) constant solid circulation rate.

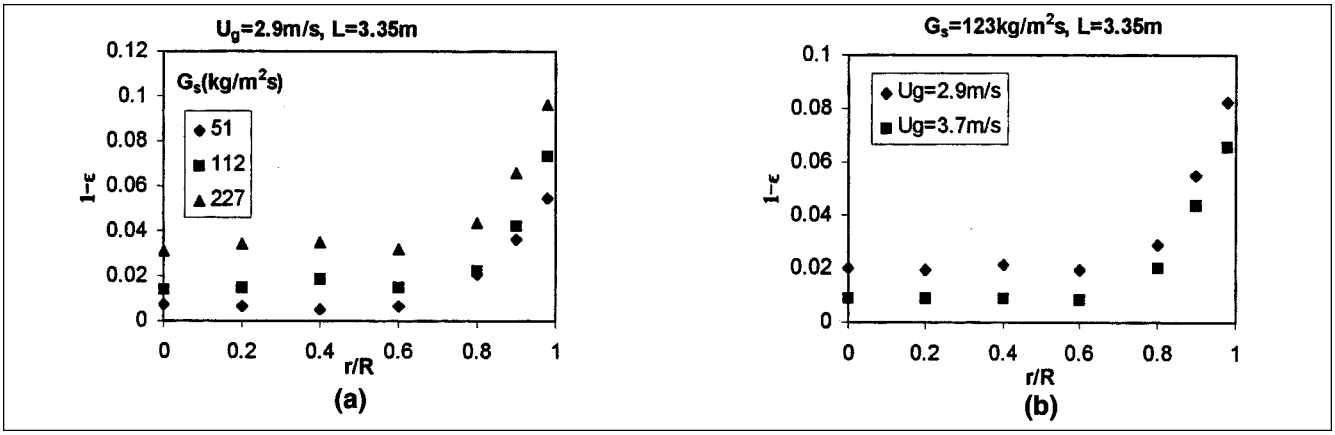

Figure 6. Radial solids density profiles.

(a) Constant gas velocity; (b) constant solid circulation rate.

achieved, although the microview (Figure 8) of the solid distribution in the downer shows a similar profile to this work. Results obtained by Herbert et al. (1994) and Bai et al. (1991) show similar solid fraction profiles, which have dense annular regions but which get dilute very close to the walls. However, the small diameter downer used by Herbert et al. (1994) usually results in strong wall region effects. The Bai et al. (1991) experiment measured the solid fraction very close to the wall, which could have a strong reflection effect on the optical fiber probe. Nevertheless, the solid fractions measured away from the wall show similar profiles to this work. In this investigation, relatively large solid/gas ratios which form a dense bed in a pilot-plant scale downer have been investigated. The core-annulus flow pattern is very clear in this unit.

The mean solids distribution along the downer axial direction is shown in Figure 9. It can be seen that the integrated solid fraction obtained from the X-ray measurements does not vary much from the top to the bottom of the downer. However, the apparent solid fraction evaluated from the pressure gradient $(1/\rho_p g)(dP/dx)$ shows negative values in the solid entrance region. The difference is caused by acceleration of solid in the entrance region. Below the entrance region, the agreement between time average X-ray measurements and time mean pressure gradient measurements is much better. Because of the restrictions imposed by the two ends of the downer, the particle acceleration in the entrance region and the deceleration in the exit region result in a relatively uniform axial solid distribution. However, the two-phase flow cannot be considered to be fully developed.

Local solids flux and particle velocity

Data collected with the local solid downflow flux measurement device are plotted in Figure 10. It shows that the solid flux is small in the central core and relatively constant. The solid flux in the wall region, however, rises sharply to a large value near the wall. This is an important difference between downer and riser flow where the high density wall region is characterized by low flux values.

Based on the information of the local values of downflow solid flux and of the solid fraction, particle velocity can be estimated by

$$U_p(r/R) = \frac{G_s(r/R)}{\rho_p[1-\epsilon(r/R)]} \tag{3}$$

Figure 11 shows the particle velocity profiles given by the above expression. The dense wall region has a much higher

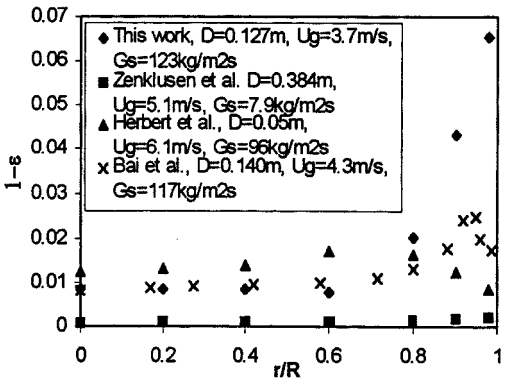

Figure 7. Comparison of solid fraction profiles obtained in different units.

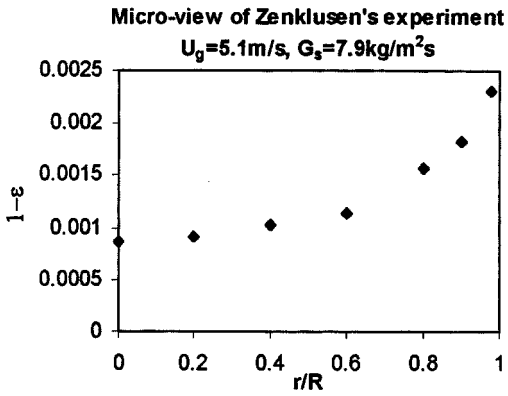

Figure 8. Micro-view of the Zenklusen et al. experimental results in a very dilute case.

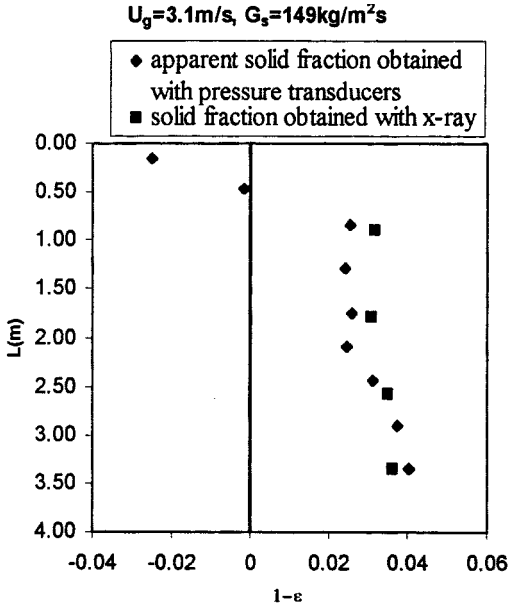

Figure 9. Axial solids density profile.

particle velocity than the dilute core in the two-phase downflow. Thus, the particle segregation and gravitational force field provide a dense, fast moving annulus and a slow, dilute core in direct contrast to riser flow. Plug-flow-like behavior could only occur in a downflow with a very dilute phase flow, since the particles move to the wall as in upflow, but speed up near the wall dragging gas along rather than slowing down. Note that the particle velocity in the core is lower than the superficial gas velocity. Since the particles move down faster than the gas, the gas velocity in the core is considerably smaller than the superficial gas velocity.

Comparison between downer and riser

The newly proposed downer reactor system has become a candidate for short residence time reactions, high solids/gas feed ratio processes, and catalytic reactions with rapid catalyst deactivation. To evaluate the performance of such a reactor, comparison between the downer and the riser is essential. The experimental data for a riser used in this comparison was obtained in a riser with a 15.2 cm inner diameter (Kostazos, 1997). Because of the relatively small geometry and dimensional differences between the two vertical systems and the differences in operating conditions, it is difficult to find identical operating conditions in the two databases on which the comparison can be conducted. However, comparisons between cases which are relatively close provide general trends which are adequate to show the dramatic differences in flow patterns between the downer and the riser.

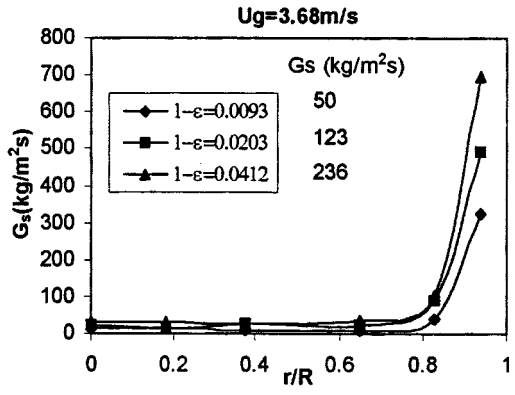

Figure 10. Solids flux profile.

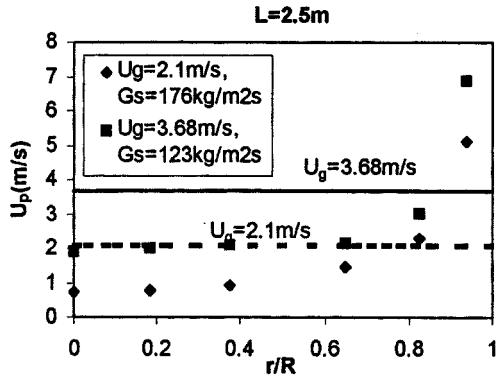

Figure 11. Estimate of local solid velocity.

In both upflow and downflow, the high velocity fluidization regime can be described with "at higher voidages and slip velocities, the continuous phase of turbulent fluidization disappears and the solids are only present as discrete particles or as ephemeral assemblages or clusters of a statistical-hydrodynamic nature" (Matsen, 1988). The general criterion for the upflow fast fluidized bed (riser) is that the bed contains both a dense phase and a dilute entrained phase above it, described as an "S-shaped" density profile (Li and Kwauk, 1980).

Axial apparent solid fraction profiles measured with differential pressure transducers in both the downer and the riser are shown in Figure 12 at the superficial gas velocity of 3.1 m/s and solid circulation rate of 149 kg/m^2·s. The positive value of the ordinate in Figure 12 represents the bed height of the riser, and the absolute value of the negative numbers represents the distances from the entrance of the downer. It can be observed that the overall axial solid fraction profile along the downer vertical column shows a much more uniform distribution than that in the riser. The dense bed in the riser entrance region and the dilute entrained phase above make up the typical riser bed. The length of the riser from the inflection point down to the entrance over which particle velocity can be changing significantly is typically much longer than that in the downer. The shorter flow developing region in the downer would better meet the kinetic requirements of relative short contact time reactions. Note that the measured negative apparent solid fraction in the entrance region of the downer is caused by the particle acceleration effect as pointed out previously.

It has been found that a core-annulus radial flow structure occurs in both the downer and the riser. In order to determine which kind of reactor behaves more plug-flow like, a comparison of radial solid fraction profiles between the downer and the riser is shown in Figure 13 at about the same distances from the bed entrances and the same operating

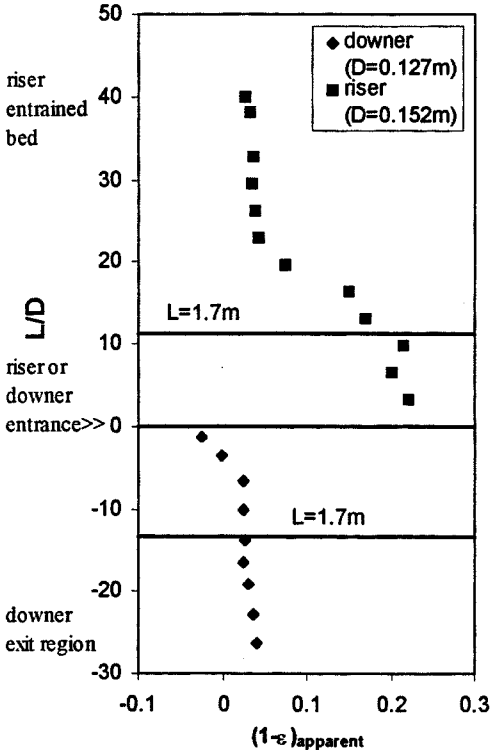

Figure 12. Axial apparent solid fraction distribution of the downer and the riser at $U_g = 3.1$ m/s, $G_s = 149$ kg/m^2·s.

conditions. It can be seen that the radial solid fraction distribution is much more uniform in the downer than in the riser. Therefore, gas-solid contact efficiency should be greatly improved in the downer as compared to the riser.

Figure 14 shows the comparison of the local solid flux in the downer and the riser. Considerable difference can be observed from this chart. Solid flux profiles measured in the downer indicate that the solid downflow flux is small in the central core and relatively constant and rises sharply to a large

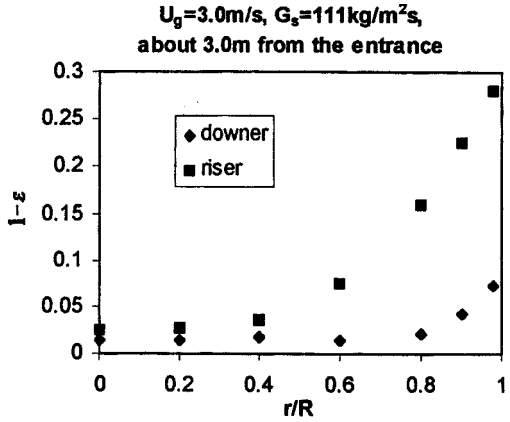

Figure 13. Radial solid fraction profiles of the downer and the riser about 3.0 m from the entrances under the same operating conditions ($U_g = 3.0$ m/s, $G_s = 111$ kg/m^2·s).

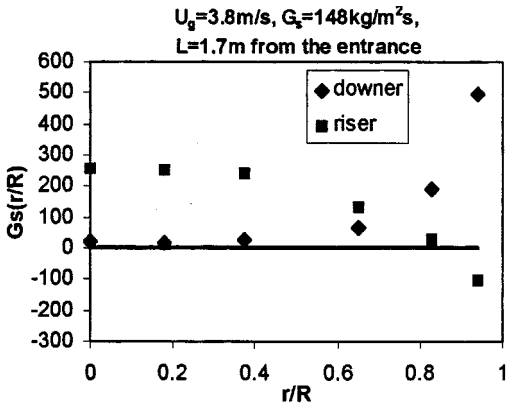

Figure 14. Solid flux profiles of the downer and the riser.

value near the wall. This is an important difference between downer and riser flow where the high density wall region is characterized by low flux values or even reversed solid flow. Solid upflow flux in the central core region of the riser has a very large value, which is in direct contrast to the small downflow flux in the core region of the downer.

Estimated values of solid velocity in the downer and riser provide the comparisons in Figure 15. They show that the riser displays a fast upflowing dilute core and slow, usually downflowing dense particle annulus. The gas near the wall of the riser is upflowing which results in large slip velocity. On the contrary, the dense wall region in the downer has much higher downflowing gas and particle velocities than does the dilute core. Thus, the particle segregation and gravitational force field provide a dense, fast-moving annulus and a slow, dilute core in direct contrast to riser flow where the dense annulus is accompanied by low particle velocity. Furthermore, higher solids concentration in the annular region of the downer leads to higher slip velocity and higher particle velocity. This is contrary to risers, where a higher slip velocity results in a reduced particle velocity.

Such flow patterns in the downer may provide a great advantage over the conventional riser in improving the product yield and selectivity. For a catalytic cracking process, the catalyst concentration is higher in the downer wall region than

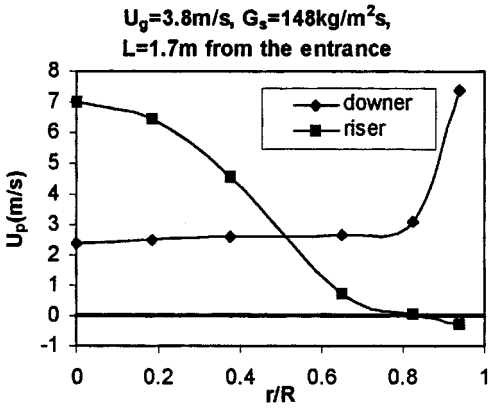

Figure 15. Solid velocity profiles of the downer and the riser.

the core region, but the residence time in the wall region is shorter than that in the core region due to the higher particle velocity in the wall region. This coupling of solid fraction with velocity should lead to more uniform cracking across the whole cross-sectional area.

Conclusions

Measurements of pressure distribution along the downflow fluidized bed show both particle acceleration and deceleration. The axial profile of solid density is quite uniform. The X-ray solid fraction measurements and local solid flux measurements indicate the existence of a core-annulus structure in the bed with a fast moving, dense annulus and a slow, dilute core. The flow developing region in which the particles accelerate is shorter in the downer than in the riser. Axial and radial gas-solids flow structures are more uniform than those in a riser. Shorter residence time but higher reaction speed in the downer wall region and longer residence time with lower reaction speed in the central region result in much more uniform reaction extent across the sectional area of the downer, and, therefore, should improve the product selectivity.

Acknowledgment

This work was supported by a National Science Foundation grant, number CTS-9312099. Exxon Research and Engineering Company was the cooperating industrial organization. W.R. Grace Co. graciously provided the cracking catalyst powder.

Notation

P = pressure in gauge, psig
r = radial coordinate, m
R = column radius, m
U_g = gas superficial velocity, m/s
U_p = particle velocity, m/s
ϵ = bed voidage
ρ_p = particle density, kg/m^3

Literature Cited

Aubert, E., D. Barreteau, T. Gauthier, and R. Pontier, "Pressure Profiles and Slip Velocities in a Co-Current Downflow Fluidized Bed Reactor," *Circulating Fluidized Bed Technology IV*, A. A. Avidan, ed., AIChE, New York, p. 403 (1994).

Bai, D. R., Y. Jin, Z. Q. Yu, and N. J. Gan, "Radial Profiles of Local Solid Concentration and Velocity in a Concurrent Downflow Fast Fluidized Bed," *Circulating Fluidized Bed Technology III*, P. Basu, M. Horio, and M. Hasatani, eds., Pergamon Press, Toronto, p. 157 (1991).

Cao, C. S., Y. Jin, Z. Q. Yu, and Z. W. Wang, "The Gas-Solids Velocity Profiles and Slip Phenomenon in a Concurrent Downflow Circulating Fluidized Bed," *Circulating Fluidized Bed Technology IV*, A. A. Avidan, ed., AIChE, New York, p. 406 (1994)

Cao, C., "Characterization of Downflowing High Velocity Fluidized Beds," PhD Thesis, The City University of New York (1998).

Feindt, H.-J., "Radial and Axial Density Fluctuations in a High Velocity Fluidized Bed," PhD Thesis, The City University of New York (1990).

Gartside, R. J., "QC—A New Reaction System," *Fluidization VI*, J. R. Grace, L. W. Shemilt, and M. A. Bergougnou, eds., Engineering Foundation, New York, p. 25 (1989).

Herbert, P. M., T. A. Gauthier, C. L. Briens, and M. A. Bergougnou, "Application of Fiber Optic Reflection Probes to the Measurement of Local Particle Velocity and Concentration in Gas-solid Flow," *Powder Technol.*, **80**, 243 (1994).

Kostazos, A., "An Investigation of the Entrance Region of a Riser Fluidized Bed," PhD Thesis, The City University of New York (1997).

Li, Y., and M. Kwauk, "The Dynamics of Fast Fluidization," *Fluidization*, J. R. Grace and J. M. Matsen, eds., Plenum Press, New York-London, p. 537 (1980).

Matsen, J. M., "The Rise and Fall of Recurrent Particles: Hydrodynamics of Circulation," *Circulating Fluidized Bed Technology II*, P. Basu and J. F. Large, eds., Pergamon Press, Toronto, p. 3 (1988).

Monceaux, L., M. Azzi, Y. Molodtsof, and J. F. Large, "Overall and Local Characterization of Flow Regimes in a Circulating Fluidized Bed," *Circulating Fluidized Bed Technology*, P. Basu, ed., Pergamon Press, Toronto, p. 185 (1985).

Murphy, J. R., "Evolutionary Design Changes Mark FCC Process," *Oil Gas J.*, **5**, 49 (1992).

Rhodes, M. J., V. S. Laussmann, and D. Geldart, "Measurements of Radial & Axial Solids Flux Variations in the Riser of a Circulating Fluidized Bed," *Circulating Fluidized Bed Technology II*, P. Basu and J. F. Large, eds., Pergamon Press, Toronto, p. 155 (1988).

Roques, Y., T. Gauthier, R. Pontier, C. L. Briens, and M. A. Bergougnou, "Residence Time Distributions of Solids in a Gas-Solids Downflow Transport Reactor," *Circulating Fluidized Bed Technology IV*, A. A. Avidan, ed., AIChE, New York, p. 555 (1994).

Schnitzlein, M. G., and H. Weinstein, "Flow Characterization in High Velocity Fluidized Beds Using Pressure Fluctuations," *Chem. Eng. Sci.*, **43**, 2605 (1988).

Shimizu, A., R. Echigo, S. Hasegawa, and M. Hishida, "Experimental Study of the Pressure Drop and the Entry Length of the Gas-Solid Suspension Flow in a Circular Tube," *Int. J. Multiphase Flow*, **4**, 53 (1978).

Wang, Z. W., D. R. Bai, and Y. Jin, "Hydrodynamics of Cocurrent Downflow Circulating Fluidized Bed (CDCFB)," *Powder Technol.*, **70**, 271 (1992).

Wei, F., Z. Wang, Y. Jin, Z. Q. Yu, and W. Chen, "Dispersion of Lateral and Axial Solids in a Cocurrent Downflow Circulating Fluidized Bed," *Powder Technol.*, **81**, 25 (1994).

Zenklusen F., R. Meili, M. Tesch, and L. Reh, "Formation of Homogeneous Downflow Gas/Solid Suspensions at High Velocities," *Circulating Fluidized Bed Technology V*, M. Kwauk, ed., Science Press, Beijing, p. 84 (1997).

Manuscript received May 15, 1999, and revision received Nov. 1, 1999.